JOURNAL OF PHYSIOLOGY AND PHARMACOLOGY 2017, 68, 2, 283-293
www.jpp.krakow.pl

A. POLUS[1], M. BOCIAGA-JASIK[2], U. CZECH[1], J. GORALSKA[1], U. CIALOWICZ[1], M. CHOJNACKA[1], M. POLUS[3], K. JUROWSKI[4], A. DEMBINSKA-KIEC[1]

THE HUMAN IMMUNODEFICIENCY VIRUS (HIV1) PROTEASE INHIBITOR SANQUINAVIR ACTIVATES AUTOPHAGY AND REMOVES LIPIDS DEPOSITED IN LIPID DROPLETS

[1]Department of Clinical Biochemistry Jagiellonian University Medical College; Cracow, Poland;
[2]Department of Gastroenterology, Hepatology and Infectious Diseases, Jagiellonian University Medical College, Cracow, Poland;
[3]Institute of Water Supply and Environmental Protection, Faculty of Environmental Engineering, Cracow University of Technology, Cracow, Poland; [4]Department of Analytical Chemistry, Faculty of Chemistry, Jagiellonian University, Cracow, Poland

Reduction in mortality and increased average life span of the human immunodeficiency virus (HIV)-infected patients treated with antiretroviral therapy (ART) are associated with the risk of unwanted effects, such as insulin resistance and dyslipidemia with cardiovascular complications. Antiretroviral therapy may also be associated with lipodystrophy characterized as peripheral lipoatrophy with central fat accumulation. Understanding the molecular mechanisms of lipodystrophy caused by ART is important for therapeutic strategy and the prediction of side-effects. Influence of protease inhibitor saquinavir (SQV) on preadipocyte differentiation was analyzed in *in vitro* human Chub-S7 cell line model. For measurement of the effects of SQV the drug was added to differentiated or non-differentiated cells. The influence of SQV on changes in the profile of gene expression was verified by microarray and changes in lipid species content were analyzed using GC-MS/MS. Results were confirmed by real-time PCR and analysis of autophagy. Addition of SQV to differentiated Chub-S7 cells lead to removal of lipids deposited in lipid droplets, down-regulation of expression of transcription factors and markers of adipocyte differentiation. Antiviral activity of SQV based on its non-selective inhibition of proteases resulted in proteasome inhibition, induction of endoplasmic reticulum stress and induction of macroautophagy. This activity was accompanied by an increase in PI, PEPL, PC lipid species especially with MUFA and PUFA. Additionally up-regulation of miR-100-3p, miR-222-5p, miR-483-5p were found, which correlated with obesity, insulin resistance, increasing insulin secretion and activation of lipolysis. Our results indicated that SQV, by inhibition of proteasome protein degradation, activated the unfolded protein response resulting in autophagic breakdown of lipids deposited in adipose tissue causing lipodystrophy.

Key words: *adipogenesis, lipidomics, microarray, autophagy, miRNA, saquinavir*

INTRODUCTION

During the last decade highly active antiretroviral therapy (HAART) dramatically reduced the mortality of HIV-infected individuals. HIV protease inhibition is one of the strategic targets in recently used antiretroviral combined therapy (1). The HIV protease packaged into viral particles has aspartyl protease activity and allows cleavage of the polyproteins gag and gag-pol in HIV infected cells. Cleavage of the polyproteins leads to the production of proteins that contribute to the structure of HIV virion packaging (2, 3). HIV protease inhibitors (PIs) prevent cleavage of gag and gag-pol protein precursors and in that way block the infectivity of nascent virions but could also inhibit intracellular protease activity.

Unfortunately, reduction in mortality of HIV-infected patients treated with HAART is associated with the risk for side effects including metabolic disorders (4-6). Preadipocytes accumulating triglycerides (TG) in lipid droplets (LDs) play an important role in protecting other cells from lipotoxic effect of ectopic lipid accumulation, preventing their destructive effect on tissue cells such as vascular endothelium, pancreatic beta cells and hepatocytes. Studies of adipose tissue collected from untreated patients infected with HIV showed a number of changes that are likely to become an initiation of the development of lipodystrophy aggravated after the introduction of PIs. Use of HIV protease inhibitors, is associated with progress of lipodystrophy characterized by peripheral lipoatrophy with central fat accumulation (7, 8). Adipose cell dysfunction during lipodystrophy includes: inhibition of adipocyte differentiation, decreased cell survival, changes in adipokine secretion, mitochondrial dysfunction and impaired recovery from oxidative stress (9-13). Inhibition of adipogenesis leads to life-threatening consequences, development of metabolic diseases (insulin resistance, non-alcoholic fatty liver disease (NAFLD), diabetes type 2, atherosclerosis, hypertension) (14-16). Therefore, understanding the molecular mechanisms of lipodystrophy induced by PIs is very important for a therapeutic strategy and in the prediction of side effects. In this study the effect of saquinavir (SQV) on changes in the profile of gene expression as well as lipid metabolism using

'high throughput methods' were analyzed. Using the differentiated Chub-S7 cell *in vitro* model allowed to analyze the decrease of lipids in lipid droplets caused by SQV lipodystrophy without the influence of environmental factors (diet, pathologies, medication therapy).

Understanding the correlation between changes in lipid profile and gene expression as molecular basis of lipodystrophy caused byPIs would allow for the detection of lipodystrophy early markers to prevent metabolic side effects enhanced during the disappearance of adipose tissue. This can be helpful in the selection of therapy as well as in the implementation of preventive procedures during therapy, such as the choice of diet.

MATERIAL AND METHODS

Cell type and culture conditions

The Chub-S7 immortalized, HPV-E7/hTERT expressing, human preadipocyte cell line (Darimont and Mace 2003, Darimont 2003) was obtained from Nestle Research Center. Preadipocytes were cultured in a mixture (1:1 (v/v) of DMEM (Dulbecco's Modified Eagle's Medium) (Sigma- Aldrich) and F12 (Sigma-Aldrich) culture media. Protocol of the study was approved by the Local Bioethics Committee at Jagiellonian University in Cracow, Poland.

Differentiation procedure

For differentiation cells were plated (at a density of $2 – 3 \times 10^4$ cells/cm^2) in the above mentioned media, supplemented with 10% fetal calf serum (FCS) (Gibco). At confluence cells were incubated in a serum-free DMEM/F12 medium, supplemented with 15 mM $NaHCO_3$, 17 µM D-panthotenic acid, 15 mM Hepes and 33 µM biotin, 10 µg/ml transferrin, 1 nM triiodothyronine, 850 nM insulin, 500 µg/ml fetuin added freshly (according to the protocol supplied by the Nestle Research Center for Chub-S7 cultivation). This medium was referred as the 'basal medium'.

Preadipocyte differentiation was achieved by adding 1 µM dexamethasone and 1 µM rosiglitazone to the basal medium for 15 days (according to the protocol supplied by the Nestle Research Center) (17, 18).

The saquinavir (SQV, RO-31-8959/000 MRS), pure substance, was obtained from the Roche Diagnostics GmbH (Mannheim, Germany). The drug stock solution (initially dissolved in ethanol and then made up to 1 mM in PBS) was stored at –20°C and diluted with the culture medium to the required concentration. SQV concentration used in the study (30 µM) was chosen on the basis of its cytotoxicity (19) and available data on SQV plasma concentrations in HIV-infected patients during treatment (20). The medium with freshly diluted SQV was changed every day.

To assess the effects of the drug on differentiated adipocytes described as the positive control (Ctrl(+)), 30 µM concentration of SQV was added on day 15 of differentiation (Ctrl(+)+SQV) and to non-differentiated Chub-S7 cells (Ctrl(–)+SQV) and then incubated for a further 15 days. Negative control cells (Ctrl(–)) were incubated without differentiation factors and SQV.

Oil-Red O staining

To measure lipid accumulation Oil Red O staining was performed (21). Cells were fixed with 3.7% paraformaldehyde and stained with a 0.5% solution of Oil Red O in isopropanol. Cells were then washed out with distilled water. Stained lipid droplets (LDs) were visualized using a light microscope (Olympus CK40; 10 × magnification). To determine the amount of accumulated Oil Red O in the LDs, it was eluted with isopropanol. and the absorbance measured (OD at 500 nm using 100% isopropanol as blank). The protein content in each sample was determined using the Lowry method.

Isolation of total RNA and miRNA

Following incubation with the studied compound, total RNA and miRNA (n = 3) were isolated from cells using TRIzol® Plus RNA Purification System (Thermo Fisher Scientific), and Gene Matrix Universal RNA/miRNA purification kit (EURX) according to the manufacturer's instructions. RNA and miRNA quality was assessed using the Agilent Bioanalyzer 2100 and quantified by spectrophotometry using the NanoDrop ND-1000 spectrophotometer.

Microarray hybridization - gene expression

Microarray experiments were performed using the Agilent Single Color human oligonucleotide arrays. Each separate RNA sample (n = 3) was hybridized to a single array and all expression changes were detected by the comparison with control (Ctrl(–) or Ctrl(+)) of appropriate chips using Gene Spring version 10 (Agilent Technologies).

Labeling of total RNA was done using the Quick Amp labeling kit as per the manufacturer's protocol. Briefly, using T7 promoter element coupled with oligoT primer, cDNA was generated. Subsequently, labeled cRNA was synthesized from cDNA using T7 RNA polymerase and dyes. Labeled cRNA was used for hybridization. Signal intensity of the labeled cRNA was measured by hybridization to human gene microarray. Hybridization was performed for 17 hours, rotating at a speed of 10 rpm at 65°C in an hybridization oven. The arrays were washed according to the manufacturer's recommendations and detection of the fluorescence signal was performed by the Agilent SureScan Microarray Scanner using extraction software (Agilent Technologies).

Microarray data analysis was done using the Gene Spring version 10 (Agilent Technologies). To identify differentially expressed genes and reduce noise, each data set was filtered according to several criteria.

Real-time PCR

Microarray results for selected genes were confirmed by real-time PCR. One µg of total RNA was reverse transcribed using the reverse transcription kit (High Capacity cDNA Reverse Transcription Kit Thermo Fisher Scientific) with random primers. Subsequently, cDNA was subjected to real-time PCR. Quantitative real-time polymerase chain reaction (qPCR) was performed with the QuantiTect SYBR Green PCR kit, using specific TaqMan Gene Expression Assays with a pair of specific PCR primers and a TaqMan probe with FAM (carboxyfluorescein) (Thermo Fisher Scientific). Amplification was performed using the continuous fluorescence detection 7900 HT Fast Real Time PCR system (Thermo Fisher Scientific). Expression ratio of target mRNA was normalized to the level of 18s RNA and compared with the control (Ctrl(–)). Data were analyzed using the ΔΔCT method.

For miRNA profile analysis reverse transcription Megaplex primer Pools, human set v3.0 and Taqman microRNA Reverse Transcription Kit were used. Using Taqman Array Human micro-RNA A + B TLDA cards and TaqMan Universal gene expression master mix expression was analyzed according to the manufacturer's recommendations. Expression was normalized to the level of U6 snRNA, RNU44, RNU48 and compared to the appropriate control. Data were analyzed using the ΔΔCT method using Data Assist v3.01 software (Thermo Fisher Scientific).

Lipid profile analysis

Cells for lipid analysis were scraped from a bottle on ice using appropriate buffer (< 300 µl) and homogenized. Protein quantity was determined and 100 µg of protein was taken for analysis.

Analysis of the lipid profile of Chub-S7 cells at different stages of differentiation was performed in cooperation with the center at Regensburg (Institute of Clinical Chemistry and Laboratory Medicine, University of Regensburg, Germany) by using gas chromatography/mass spectrometry as described in Leidl, Liebisch, Schmith (22-24). The content of individual classes of cellular lipids with fatty acids with different carbon chain lengths in the various lipid fractions was determined from the averaged amount of lipid/mg protein from three experiments.

Autophagy

The differentiated and non-differentiated Chub-S7 cells were cultured with SQV for 15 days on 24-well plates as described above. Autophagy was analyzed using the Autophagy/Cytotoxicity dual staining kit (Cayman Chemical) according to the manufacturer's instructions. After the treatment period cells were centrifuged and supernatant was aspirated from each well. The addition of monodansylcadaverine (MDC), a fluorescent compound incorporated into cellular multilamellar bodies by both the ion trapping mechanism and the interaction with membrane lipids, allowed to detect autophagic vacuoles in cultured cells. After 10 minutes incubation at 37°C and washing, autophagic vacuoles stained with MDC were detected with a UV filter using a plate reader. Results were presented as percent of Ctrl(–). The protein content of each sample was determined using the Lowry method.

Statistical analysis

Results from experiments for determination of gene and miRNA expression obtained from 3 experiments were expressed as mean ± S.E. (standard error) and calculated according Applied Biosystem guidelines. Two-tailed Student's t-test comparing the $2^{(-\Delta Ct)}$ values of the groups was performed for P-value calculation. Data were analyzed using Data Assist v3.01 software (Thermo Fisher Scientific). A P-value < 0.05 was considered statistically significant.

For other tests, results from three experiments were expressed as mean ± S.D. (standard deviation). Statistical significance was determined by Student's t-Test for normally distributed data using the STATISTICA v. 12 software. A P-value < 0.05 was considered statistically significant.

To identify differentially expressed genes in microarray hybridization and reduce noise, each data set of fluorescence signals was normalized using median shift algorithm (shifted to 75 percentile) with background correction to median of all samples. Only entities with normalized signals flagged as detected on 3 microarrays per condition were used for the fold of change calculation. Genes, in which expression was altered >1.5-fold were included for analysis. The fold of change was calculated in relation to Ctrl(–) or Ctrl(+) and used as expression level. A list of significantly regulated transcripts with P < 0.05 was generated using statistical filtering (one-way ANOVA followed by the Benjamini-Hochberg multiple test correction FDR and the Tukey post-hoc test) and was used for gene ontology and signaling pathways analysis. Microarray data analysis was performed using Gene Spring version 13 (Agilent Technologies) and PathVisio 3 (25).

RESULTS

Incubation of Chub-S7 cells in serum-free proadipogenic MDI medium for 48 hours promoted cell differentiation and lipid droplet formation. The maximum accumulation of lipids in Chub-S7 cells was observed after 15 days of culture (*Fig. 1*). Quantitative analysis performed after 15 days by the Oil Red O staining revealed a 2-fold increase of cellular lipid accumulation

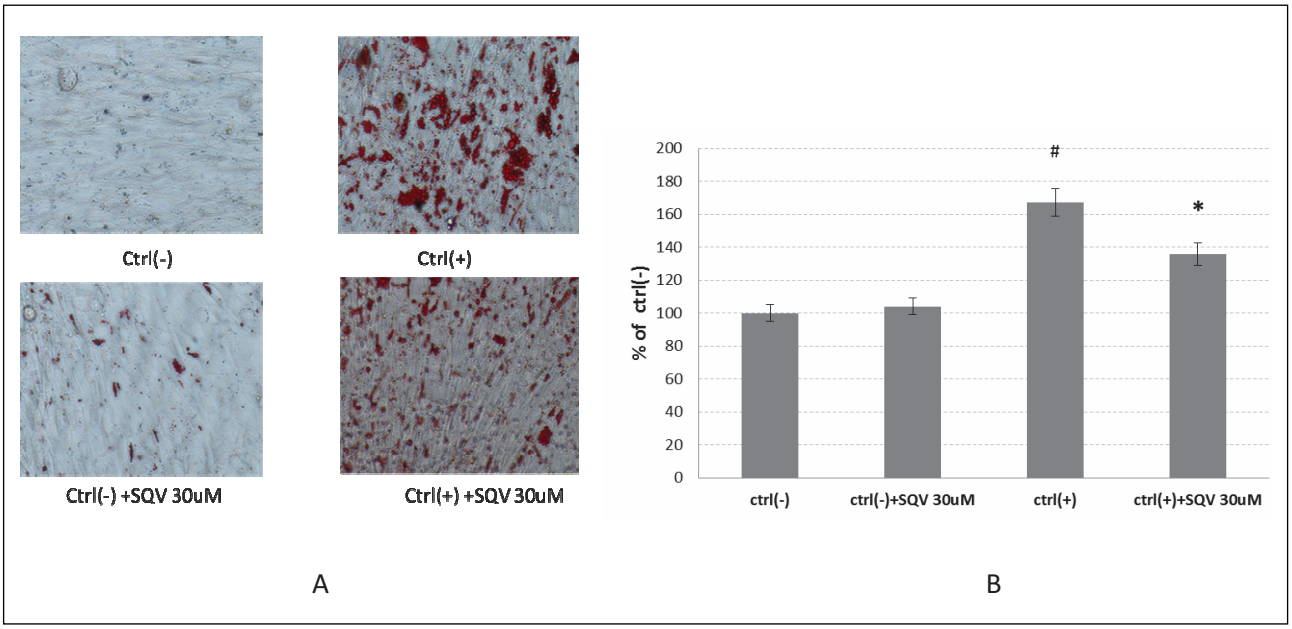

Fig. 1. Lipid accumulation (Oil-Red-O staining) in non-differentiated and differentiated Chub-S7 cells in the presence of saquinavir (SQV 30 µM). (A): LD formation in Chub-S7 cells (representative photos). (B): quantitative analysis of LD formation, data presented as percent of negative control ctrl(–). Data presented as mean ± S.D. Significant differences are indicated by asterisks, Student's t-test #P < 0.05 ctrl(–), *P < 0.05 versus ctrl(+), (n = 3, performed in triplicate).

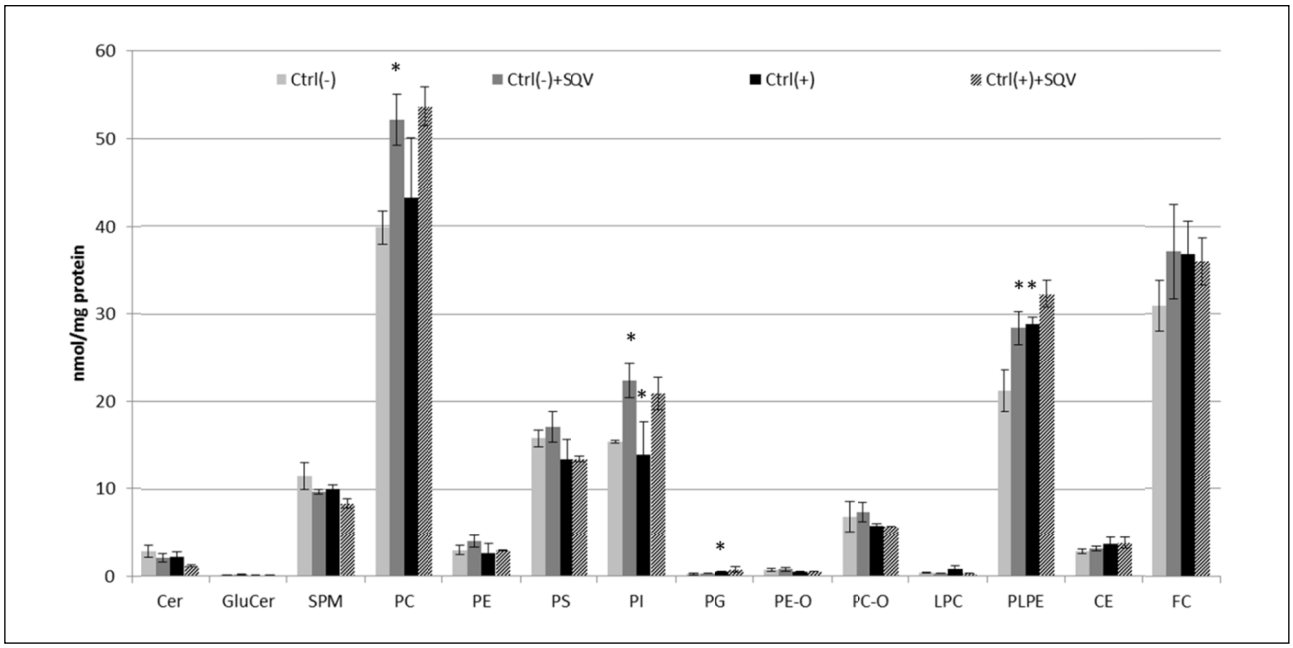

Fig. 2. Changes in lipid species content in non-differentiated and differentiated Chub-S7 cells in the presence of saquinavir (SQV 30 µM). The results are presented as average lipid species concentration (nmol/mg protein) detected using mass spectrometry GC-MS/MS (n = 3). Data presented as mean ± S.D. Significant differences are indicated by asterisks, ANOVA, Tukey post-hoc *P < 0.05 versus ctrl(–).

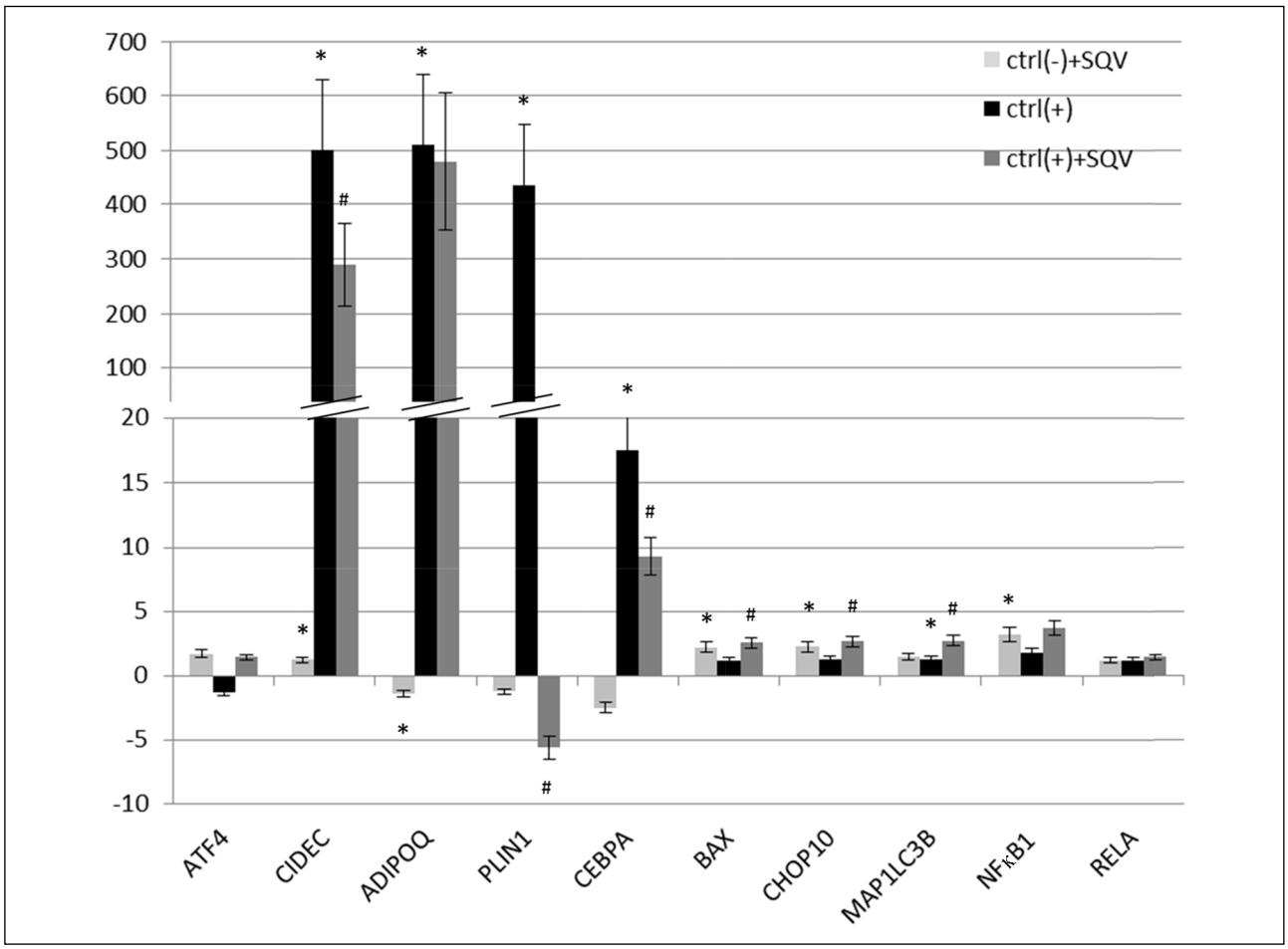

Fig. 3. Effect of SQV influence in non-differentiated and differentiated Chub-S7 cells on expression of selected genes: related to ER-stress (ATF4, CHOP10, BAX), NFκB pathway (NFκB1, RELA), adipogenesis (ADIPOQ, PLIN1, CEBPA, CIDEC) and autophagy (MAP1LC3B). Data presented as mean ± S.E. Significant differences are indicated by asterisks, Student's t-test *P < 0.05 versus ctrl(–), # P < 0.05 versus ctrl(+), (n = 3).

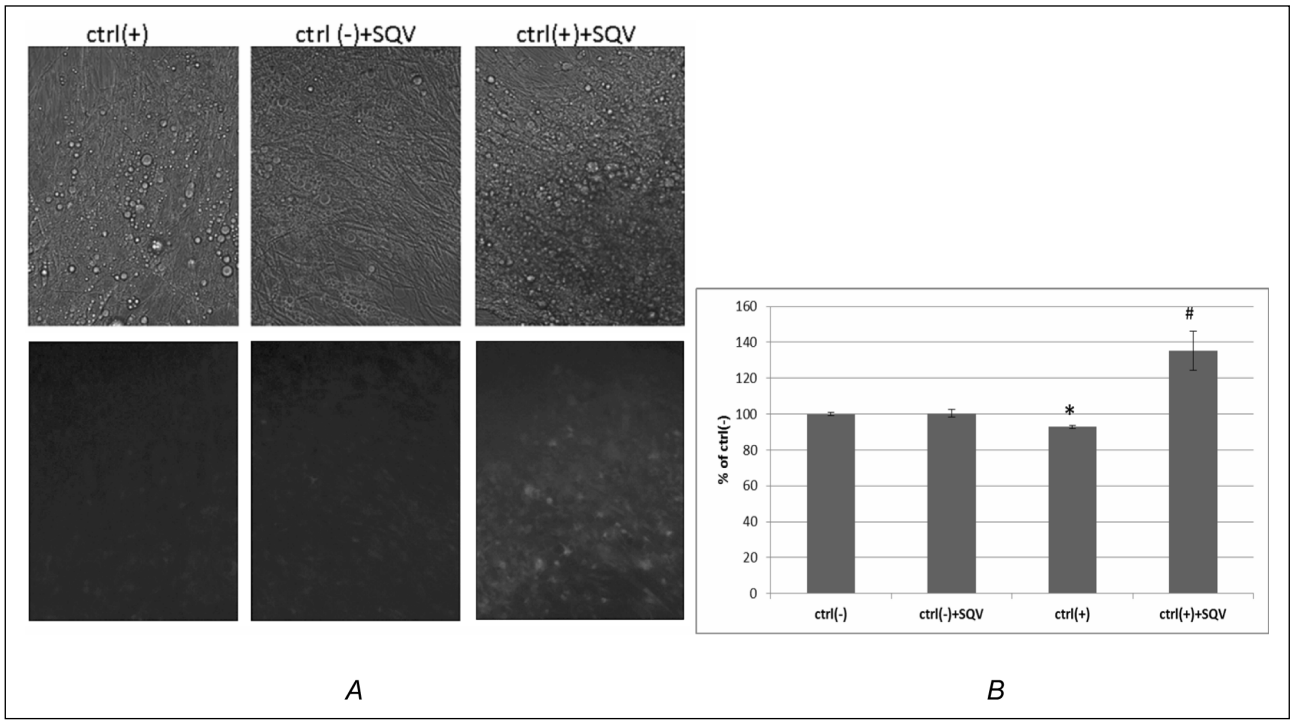

Fig. 4. Influence of SQV on autophagy in non-differentiated and differentiated Chub-S7 cells. (A) Autophagy vacuoles formation stained using MDC in Chub-S7 cells (representative photos). (B) Quantitative analysis of fluorescence intensity of MDC stained Chub-S7 cells, data presented as percent of ctrl(–). Significant differences are indicated by asterisks, Student's ttest *P < 0.05 versus ctrl(–), #P < 0.05 verus ctrl(+), (n = 3).

in LDs (*Fig. 1*). SQV alone did not influence the lipid accumulation. Adding 30 μM of SQV to previously differentiated Chub-S7 cells decreased lipid content in LDs.

For the analysis of changes in the lipidome in non-differentiated and differentiated Chub-S7 cells in the presence of SQV (30 μM), cell homogenates corresponding to 100 μg of protein were subjected to lipid species analysis by GC-MS/MS for the following lipid classes: phosphatidylcholine (PC), lysophosphatidylcholine (LPC), phosphatidylethanolamine (PE), PE-based plasmalogen (PEPL), phosphatidylglycerol (PG), phosphatidylinositol (PI), sphingomyelin (SPM), ceramide (Cer), free cholesterol (FC) and cholesteryl esters (CE).

The predominant lipid classes in Chub-S7 cells were PC and FC. Incubation of non-differentiated Chub-S7 cells with SQV (Ctrl(–)+SQV) increased the content of PI, PPL, PC. The differentiation resulted in the formation of microscopically visible LDs and in a statistically significant change in PG, PEPL, PI (analysis Ctrl(+) versus Ctrl(–)). Addition of SQV to differentiated cells increased PI, PEPL, PC but these changes did not reach significance level (analysis Ctrl(+)+SQV versus Ctrl(+)) (*Fig. 2*).

Analysis of fatty acids content in two lipid species: cholesterol esters, accumulated in LDs and plasmalogens membrane phospholipids, cellular source of PUFAs (polyunsaturated fatty acids), demonstrated that differentiation stimulating conditions elevated content of saturated fatty acids (SFA). Addition of SQV to non-differentiated and differentiated Chub-S7 cells elevated mainly MUFA and PUFA (*Table 2*).

Microarray results analysis indicated that differentiation caused a statistically significant increase in expression of the transcription factors - master players of preadipocyte differentiation such as: CEBPD, CEBPA, PPARγ, PGC1A, NR1H3, and markers of adipocyte differentiation PLIN1, PLIN5, CIDEC, AGPAT2, LPL, ADIPOQ, SLC2A4 (*Table 1*). There was also established effect of the used proadipogenic condition on up-regulation of the TCA cycle, beta-oxidation enzymes. Differentiation of preadipocytes was associated with the up-regulation of the expression of ACSL1, ACSL2 enzymes that convert free long-chain fatty acids into fatty acyl-CoA esters and allows lipid biosynthesis or fatty acid catabolism. The increased gene expression of ACACB - enzyme participating in synthesis of malonylo-CoA, and elongase ELOVL5 was observed. We found up-regulation of GPD1, GPAM AGPAT2, PPAP2A, DGAT2 genes coding for enzymes participating in elevation of DAG and TG synthesis (*Table 2*). Adding SQV to non-differentiated and differentiated Chub-S7 cells generally had an opposite effect (*Table 1*) namely decreased expression of adipogenesis activating genes.

Antiviral activity of SQV has the ability to reduce HIV protease activity but could also inhibit proteases in host cells. This resulted in inhibition of proteasome activity leading to the accumulation of protein, aggregates formation, induction of endoplasmic reticulum stress and apoptosis. The formed aggregates could be broken down during macroautophagy.

In our study the addition of SQV to differentiated Chub-S7 cells up-regulated gene expression of proteins participating in different stages of autophagy: autophagosome formation (MAP1LC3B, SQSTM1, WIPI2, ATG2A, ATG4B, ATG4D, ATG16L1, FEZ1), autophagosome maturation (LAMP1) and fusion with lysosomes (VTI1A, EVA1A, NSF, CTSB), which confirmed autophagy activation (26). The observed decrease in mitochondrial gene expression (TOM-20, COX proteins building mitochondrial IV cytochrome C oxidase complex *etc*.) indicated mitophagy activation (*Table 1*) (26).

The results obtained by microarray gene expression were verified for selected genes by real-time PCR. Generally, real-time gene expression analysis confirmed microarray results (*Fig. 3*).

The biological interpretation of microarray results related to the influence of SQV on autophagy was empirically verified

Table 1. Changes in the gene expression of proteins in non-differentiated and differentiated Chub-S7 cells in the presence of saquinavir (SQV 30 μM) (microarray (Agilent), n = 3, one-way ANOVA followed by Benjamini-Hochberg multiple test correction FDR and Tukey post-hoc test, ratio with P < 0.05 in post-hoc test- bolded).

GeneSymbol	P (Corr)	P	ctrl(-) +SQV vs ctrl(-)	ctrl(+) vs ctrl(-)	ctrl(+) +SQV vs ctrl(-)	ctrl(+) +SQV vs ctrl(+)	EnsemblID	EntrezGeneID	RefSeq
adipogenesis									
ADIPOQ	7.86E-04	5.14E-06	2.2	**166.3**	5.1	**-32.5**	ENST00000444204	9370	NM_004797
CD36	1.52E-02	6.18E-04	-1.1	**30.8**	6.4	-4.8	ENST00000419819	948	NM_001001547
CEBPA	6.51E-07	1.24E-10	-1.0	**118.3**	**13.2**	**-9.0**	ENST00000498907	1050	NM_004364
CFD	1.35E-02	5.11E-04	1.7	**36.0**	**9.6**	-3.7	ENST00000617994	1675	NM_001928
GTF3A	5.98E-03	1.41E-04	1.2	1.2	**1.6**	**1.3**	ENST00000439403	2971	NM_002097
HSD11B2	3.52E-03	6.05E-05	2.2	**17.2**	**3.2**	**-5.4**	ENST00000326152	3291	NM_000196
LIPE	7.36E-09	4.35E-13	**1.5**	**84.2**	**6.1**	**-13.9**	ENST00000244289	3991	NM_005357
LPL	1.24E-06	2.92E-10	1.2	**542.7**	**15.9**	**-34.0**	ENST00000311322	4023	NM_000237
MBNL1	4.13E-03	7.66E-05	1.0	-1.2	**-2.2**	**-1.8**	ENST00000485910	4154	NM_021038
MEF2A	7.05E-03	1.84E-04	-1.1	1.0	**-1.8**	**-1.9**	ENST00000449277	4205	NM_001171894
MEF2C	2.03E-02	9.53E-04	-1.3	1.3	**-5.8**	**-7.6**	ENST00000510942	4208	NM_002397
MEF2D	1.01E-03	7.69E-06	-1.3	**-2.9**	**-2.3**	1.3	ENST00000348159	4209	NM_005920
NCOA1	1.33E-03	1.17E-05	1.2	**1.7**	**-1.5**	**-2.6**	ENST00000395856	8648	NM_147233
NR1H3	4.73E-02	3.42E-03	1.4	**4.6**	2.8	-1.7	ENST00000407404	10062	NM_005693
NRIP1	1.25E-02	4.50E-04	-1.0	**2.0**	-1.4	**-2.8**	ENST00000318948	8204	NM_003489
PPARG	8.27E-03	2.35E-04	1.3	**5.0**	**2.1**	**-2.4**	ENST00000396999	5468	NM_138711
PPARGC1A	2.12E-02	1.02E-03	1.1	**9.0**	2.0	**-4.6**	ENST00000264867	10891	NM_013261
RXRG	4.19E-03	7.85E-05	1.2	**6.6**	1.1	**-6.0**	ENST00000470566	6258	NM_006917
SLC2A4	6.22E-03	1.51E-04	-1.4	**6.4**	-1.0	**-6.6**	ENST00000317370	6517	NM_001042
SPOCK1	2.08E-03	2.59E-05	-1.2	**-2.1**	**-4.2**	**-2.0**	ENST00000282223	6695	NM_004598
fatty acids synthesis									
ACAA2	3.58E-03	6.27E-05	1.1	**4.1**	1.8	**-2.3**	ENST00000591171	10449	NM_006111
ACACB	4.69E-05	6.11E-08	-1.2	**17.6**	**1.6**	**-11.2**	ENST00000538526	32	NM_001093
ACSL1	3.43E-06	1.22E-09	1.2	**19.3**	**4.5**	**-4.3**	ENST00000281455	2180	NM_001995
ACSS2	1.65E-02	7.01E-04	1.4	**4.5**	**2.0**	**-2.2**	ENST00000360596	55902	NM_018677
ECHDC1	5.57E-04	2.79E-06	-1.3	**2.1**	-1.3	**-2.7**	ENST00000488087	55862	NM_018479
ECHDC2	4.42E-02	3.10E-03	1.1	1.2	-1.3	**-1.6**	ENST00000358358	55268	NM_018281
ECHS1	2.44E-03	3.34E-05	1.0	**1.9**	**1.5**	-1.3	ENST00000368547	1892	NM_004092
ELOVL5	1.17E-03	9.61E-06	-1.1	**1.9**	**-1.5**	**-2.9**	ENST00000304434	60481	NM_021814
HADHB	3.40E-02	2.08E-03	1.2	**2.8**	1.6	-1.7	ENST00000434972	3032	NM_001281513
MECR	2.30E-03	3.04E-05	1.1	**1.5**	**1.8**	1.2	ENST00000478505	51102	NM_001024732
PC	4.44E-04	1.98E-06	-1.3	**3.0**	-1.1	**-3.2**	ENST00000393960	5091	NM_001040716
PECR	1.08E-04	2.25E-07	-1.0	**5.0**	**2.3**	**-2.2**	ENST00000461330	55825	NM_018441
TG synthesis									
AGPAT2	7.43E-04	4.63E-06	1.1	**3.5**	1.5	**-2.4**	ENST00000538402	10555	NM_006412
DGAT2	9.68E-05	1.92E-07	1.2	**17.2**	**2.8**	**-6.2**	ENST00000603363	84649	NM_032564
DGAT1	2.88E-02	1.61E-03	-1.0	**1.7**	**1.6**	-1.1	ENST00000524965	8694	NM_012079
GPAM	9.68E-05	1.93E-07	1.3	**17.4**	1.8	**-9.6**	ENST00000348367	57678	NM_020918
GPD1	3.16E-03	5.02E-05	-1.5	**22.3**	1.2	**-17.9**	ENST00000301149	2819	NM_005276
MGAT2	4.20E-02	2.87E-03	1.1	**-1.5**	**-1.6**	-1.0	ENST00000305386	4247	NM_002408
PNPLA2	8.16E-04	5.48E-06	1.2	**11.7**	1.8	**-6.6**	ENST00000529255	57104	NM_020376
PPAP2A	3.33E-02	2.02E-03	1.5	**2.6**	1.5	**-1.7**	ENST00000307259	8611	NM_176895
PPAP2B	4.17E-03	7.77E-05	1.2	-1.7	**-3.1**	**-1.8**	ENST00000371250	8613	NM_003713
lipid droplets formation									
LIPC	2.19E-02	1.07E-03	1.5	-2.1	**-5.3**	-2.6	ENST00000356113	3990	NM_000236
LIPE	7.36E-09	4.35E-13	**1.5**	**84.2**	**6.1**	**-13.9**	ENST00000244289	3991	NM_005357
LPL	1.24E-06	2.92E-10	1.2	**542.7**	**15.9**	**-34.0**	ENST00000311322	4023	NM_000237
LRP1	9.15E-03	2.76E-04	1.1	1.1	-2.2	**-2.4**	ENST00000556356	4035	NM_002332
ARFGAP1	1.12E-02	3.75E-04	-1.3	**-1.6**	-1.0	**1.5**	ENST00000370275	55738	NM_175609
LDLR	2.65E-02	1.42E-03	1.2	**-1.8**	-1.6	**1.1**		3949	NM_000527
LEPR	0.030757198	0.001783395	1.0	2.0	-2.3	**-4.5**	ENST00000344610	3953	NM_001198688
CIDEC	1.37E-03	1.23E-05	2.8	**43.1**	**7.4**	**-5.8**	ENST00000336832	63924	NM_022094
CIDEA	2.83E-02	1.57E-03	-2.0	2.7	-2.0	**-5.5**	ENST00000320477	1149	NM_001279
CPT1B	2.73E-03	3.90E-05	1.6	**5.2**	**2.2**	**-2.4**	ENST00000360719	1375	NM_152246
CPT1C	9.16E-04	6.56E-06	1.2	**-2.4**	-1.0	**2.3**	ENST00000598293	126129	NM_001199752
PLIN1	6.38E-03	1.57E-04	1.1	**51.6**	3.3	**-15.5**	ENST00000430628	5346	NM_002666
PLIN5	4.54E-02	3.22E-03	1.2	**10.4**	3.0	-3.4	ENST00000381848	440503	NM_001013706
PNPLA2	8.16E-04	5.48E-06	1.2	**11.7**	1.8	**-6.6**	ENST00000529255	57104	NM_020376
NSF	9.61E-03	3.02E-04	1.0	**-1.9**	-1.4	**1.4**	ENST00000611398	4905	NM_006178
RAB35	1.96E-03	2.37E-05	1.0	1.1	**1.9**	**1.7**	ENST00000229340	11021	NM_006861
SEC22A	2.02E-02	9.45E-04	1.2	-1.0	**1.9**	**2.0**	ENST00000309934	26984	NM_012430
mitochondrial function related genes									
BCS1L	4.92E-04	2.38E-06	**1.2**	**1.3**	2.0	**1.5**	ENST00000439945	617	NM_004328
CYC1	4.68E-04	2.20E-06	-1.1	**2.4**	**2.0**	-1.2	ENST00000528618	1537	NM_001916
OPA1	5.57E-03	1.27E-04	-1.3	-1.0	**-2.3**	**-2.3**	ENST00000495261	4976	NM_130837
SLC25A4	6.21E-03	1.50E-04	-1.1	**2.0**	**1.5**	-1.3	ENST00000491736	291	NM_001151
TOMM20	4.75E-02	3.44E-03	-1.0	1.5	-1.4	**-2.1**	ENST00000366607	9804	NM_014765
ND1	1.10E-02	3.66E-04	-1.0	**2.4**	1.0	**-2.4**	ENST00000361390	4535	BC061915
ND2	2.96E-02	1.67E-03	1.0	**2.2**	**1.7**	-1.3	ENST00000361453	4536	HW291277
ND3	1.93E-02	8.85E-04	1.0	**1.3**	**1.6**	1.2	ENST00000361227	4537	HV963894
NDUFA6	3.82E-03	6.80E-05	-1.1	**1.5**	**1.3**	-1.2	ENST00000605927	4700	NM_002490
NDUFB9	6.24E-04	3.42E-06	-1.1	**1.6**	**1.3**	**-1.2**	ENST00000518657	4715	NM_005005
NDUFA9	3.96E-04	1.69E-06	1.2	**1.6**	**1.8**	1.1	ENST00000544675	4704	NM_005002
NDUFB5	5.07E-03	1.10E-04	1.1	**2.2**	1.2	**-1.8**	ENST00000477177	4711	NM_001199958
NDUFV3	5.40E-05	7.55E-08	1.2	**2.4**	**2.9**	1.2	ENST00000460259	4731	NM_021075
NDUFS7	2.54E-03	3.51E-05	1.0	**1.9**	**1.5**	-1.2	ENST00000538929	374291	NM_024407
NDUFS8	1.12E-02	3.78E-04	1.0	**1.8**	**2.0**	1.1	ENST00000313468	4728	NM_002496
NDUFV1	1.80E-04	5.39E-07	1.1	**2.0**	**1.7**	-1.2	ENST00000531250	4723	NM_007103

NDUFS1	2.75E-03	3.95E-05	1.1	**1.8**	1.2	**-1.5**	ENST00000449699	4719	NM_005006
SDHB	2.10E-04	6.57E-07	-1.0	**1.7**	**1.6**	-1.0	ENST00000475506	6390	NM_003000
SDHC	3.33E-02	2.03E-03	1.1	**-1.6**	1.1	**1.8**	ENST00000367975	6391	NM_003001
SDHD	1.07E-03	8.31E-06	-1.1	**1.4**	-1.1	**-1.5**	ENST00000530923	6392	NM_003002
UQCRC1	8.54E-03	2.45E-04	1.1	**2.1**	**2.3**	1.1	ENST00000415995	7384	NM_003365
UQCRC2	2.79E-03	4.10E-05	1.1	**2.1**	1.3	**-1.6**	ENST00000563898	7385	NM_003366
UQCRH	2.08E-03	2.60E-05	1.0	**1.7**	**1.5**	**-1.1**	ENST00000483273	7388	NM_006004
UQCR10	2.96E-02	1.67E-03	-1.0	**1.4**	**1.6**	**1.2**	ENST00000401406	29796	NM_001003684
UQCRFS1	2.72E-04	9.93E-07	1.0	**1.9**	**1.6**	-1.2	ENST00000304863	7386	NM_006003
COX6A1	8.99E-03	2.67E-04	1.1	**1.5**	**1.6**	1.1	ENST00000549525	1337	NM_004373
COX7A2	1.51E-02	6.10E-04	1.0	**1.4**	**1.5**	1.0	ENST00000459637	1347	NM_001865
COX7B	1.22E-02	4.32E-04	-1.1	**1.9**	1.3	**-1.5**	ENST00000373335	1349	NM_001866
ATP5B	6.67E-04	3.81E-06	1.1	**2.1**	**1.5**	**-1.4**	ENST00000550162	506	NM_001686
ATP5D	1.04E-02	3.39E-04	1.0	**1.6**	**1.3**	-1.2	ENST00000590265	513	NM_001001975
ATP5F1	1.18E-03	9.80E-06	1.0	**1.7**	**1.3**	**-1.3**	ENST00000468818	515	NM_001688
ATP5G2	7.77E-04	4.99E-06	1.0	**1.5**	**1.4**	-1.1	ENST00000549164	517	NM_001002031
ATP5G3	3.01E-03	4.69E-05	1.2	**1.9**	**1.9**	-1.0	ENST00000497075	518	NM_001002258
ATPIF1	3.77E-03	6.68E-05	-1.1	**-1.8**	-1.2	**1.5**	ENST00000335514	93974	NM_016311
SLC25A6	1.25E-03	1.08E-05	-1.2	**1.9**	1.1	**-1.8**	ENST00000381401	293	NM_001636
SAMM50	1.50E-04	3.88E-07	1.2	**2.2**	**1.7**	**-1.3**	ENST00000494795	25813	NM_015380
TIMM22	1.46E-02	5.75E-04	1.1	1.2	**1.7**	**1.4**	ENST00000613269	29928	NM_013337
TIMM50	3.28E-03	5.41E-05	-1.0	1.4	**2.2**	**1.6**	ENST00000607714	92609	NM_001001563
TIMM17B	3.39E-02	2.07E-03	1.0	1.5	**1.9**	1.2	ENST00000466995	10245	NM_001167947
TIMM21	3.42E-02	2.09E-03	1.1	**1.5**	**1.6**	1.1	ENST00000169551	29090	NM_014177
TIMM44	4.50E-04	2.01E-06	1.1	**2.5**	**2.4**	-1.0	ENST00000595876	10469	NM_006351
HSPA9	1.11E-02	3.72E-04	-1.2	**1.9**	1.5	-1.3	ENST00000297185	3313	NM_004134
GRPEL2	2.82E-02	1.56E-03	1.2	**1.5**	**1.8**	1.2	ENST00000507562	134266	NM_152407
TIMM13	9.25E-03	2.82E-04	-1.1	**2.2**	-1.0	**-2.2**	ENST00000215570	26517	NM_012458
TIMM8B	5.89E-04	3.18E-06	1.1	1.2	**1.7**	**1.5**	ENST00000507614	26521	NM_012459
UCP2	7.65E-04	4.88E-06	1.1	**11.2**	**3.8**	**-2.9**	ENST00000310473	7351	NM_003355
beta-oxidation									
ACADM	9.83E-03	3.13E-04	-1.1	**3.0**	-1.3	**-3.8**	ENST00000420607	34	NM_000016
ACADS	8.66E-03	2.52E-04	-1.0	**5.0**	2.3	-2.2	ENST00000242592	35	NM_000017
ACAT1	2.98E-02	1.70E-03	-1.1	**1.7**	-1.1	**-1.9**	ENST00000533610	38	NM_000019
ACSL1	3.43E-06	1.22E-09	1.2	**19.3**	**4.5**	**-4.3**	ENST00000281455	2180	NM_001995
ACSS2	1.65E-02	7.01E-04	1.4	**4.5**	**2.0**	**-2.2**	ENST00000360596	55902	NM_018677
ACSL1	3.43E-06	1.22E-09	1.2	**19.3**	**4.5**	**-4.3**	ENST00000281455	2180	NM_001995
CHKB	1.19E-02	4.19E-04	1.1	**1.7**	1.1	**-1.5**	ENST00000468532	1120	NM_005198
ACADL	3.75E-02	2.40E-03	-1.5	**2.7**	2.0	-1.3	ENST00000233710	33	NM_001608
ECHS1	2.44E-03	3.34E-05	1.0	**1.9**	**1.5**	-1.3	ENST00000368547	1892	NM_004092
CPT1B	2.73E-03	3.90E-05	1.6	**5.2**	**2.2**	**-2.4**	ENST00000360719	1375	NM_152246
CPT2	1.58E-03	1.66E-05	1.2	**2.5**	**2.4**	-1.1	ENST00000371486	1376	NM_000098
HADH	8.70E-03	2.54E-04	1.0	**3.2**	1.5	**-2.1**	ENST00000603302	3033	NM_005327
HADHB	3.40E-02	2.08E-03	1.2	**2.8**	1.6	-1.7	ENST00000434972	3032	NM_001281513
SLC25A20	1.72E-02	7.45E-04	1.5	**3.5**	**3.0**	-1.2	ENST00000440964	788	NM_000387
TCA									
ACO2	6.51E-07	1.28E-10	1.1	**3.4**	**1.7**	**-2.0**	ENST00000216254	50	NM_001098
CS	1.73E-04	4.96E-07	1.1	**2.3**	1.1	**-2.2**	ENST00000351328	1431	NM_004077
IDH3B	9.25E-03	2.82E-04	1.0	**1.5**	**1.3**	-1.1	ENST00000479376	3420	NM_174855
IDH3G	1.39E-03	1.26E-05	1.1	**1.8**	1.2	**-1.5**	ENST00000619865	3421	NM_004135
DLST	1.41E-02	5.48E-04	1.4	**2.0**	**2.6**	1.3	ENST00000334220	1743	NM_001933
IDH3A	9.47E-03	2.94E-04	1.0	**3.6**	**2.7**	-1.3	ENST00000558535	3419	NM_005530
MDH2	3.92E-05	3.63E-08	1.1	**1.6**	**1.9**	1.1	ENST00000424167	4191	NM_005918
SDHB	2.10E-04	6.57E-07	-1.0	**1.7**	**1.6**	-1.0	ENST00000475506	6390	NM_003000
SDHC	3.33E-02	2.03E-03	1.1	**-1.6**	1.1	**1.8**	ENST00000367975	6391	NM_003001
SUCLG1	1.39E-03	1.25E-05	-1.0	**1.9**	**1.5**	-1.2	ENST00000487809	8802	NM_003849
SUCLG2	1.59E-02	6.59E-04	-1.1	-1.0	**-1.9**	**-1.9**	ENST00000307227	8801	NM_003848
apoptosis									
BAK1	7.97E-04	5.28E-06	-1.0	1.2	**2.4**	**2.0**	ENST00000374467	578	NM_001188
BAX	2.51E-02	1.30E-03	-1.2	**-1.8**	1.1	**1.9**	ENST00000513545	581	NM_138764
BIK	1.51E-02	6.10E-04	2.2	1.1	**6.7**	**5.9**	ENST00000216115	638	NM_001197
BCL2L1	1.08E-04	2.29E-07	**1.6**	**2.2**	**3.2**	**1.4**	ENST00000307677	598	NM_138578
BNIP3L	1.53E-03	1.58E-05	-1.2	-1.2	**-1.9**	**-1.6**	ENST00000620910	665	NM_004331
BOK	5.68E-05	8.40E-08	-1.0	**2.1**	1.2	**-1.8**	ENST00000318407	666	NM_032515
CASP6	3.17E-03	5.06E-05	1.2	**-1.6**	1.2	**2.0**	ENST00000505117	839	NM_001226
CASP10	2.16E-04	6.92E-07	**1.3**	**-1.3**	**1.8**	**2.3**	ENST00000346817	843	NM_032977
CYCS	3.48E-02	2.16E-03	-1.2	**1.8**	1.0	**-1.7**		54205	NM_018947
DIABLO	2.37E-02	1.19E-03	1.1	1.1	**1.6**	**1.4**	ENST00000535844	56616	NM_019887
TNFSF10	3.60E-02	2.27E-03	1.4	**-2.7**	-1.5	**1.7**	ENST00000241261	8743	NM_003810
TNFRSF25	8.99E-03	2.67E-04	1.2	**-2.4**	-1.7	1.4	ENST00000513135	8718	NM_148965
autophagy									
BAG1	3.23E-02	1.93E-03	-1.1	**1.8**	1.5	-1.2	ENST00000468274	573	NM_001172415
FEZ1	1.39E-03	1.3E-05	1.3	-1.2	2.1	**2.6**	ENST00000528863	9638	NM_005103
ATG16L1	2.55E-02	1.34E-03	1.2	**1.3**	**1.6**	**1.2**	ENST00000474148	55054	NM_030803
ATG2A	3.07E-02	1.78E-03	-1.1	**-1.6**	1.2	**2.0**	ENST00000421419	23130	NM_015104
BCL2L1	1.08E-04	2.29E-07	**1.6**	**2.2**	**3.2**	**1.4**	ENST00000307677	598	NM_138578
CTSB	1.77E-03	2.01E-05	-1.1	**-4.7**	-1.5	**3.2**	ENST00000353047	1508	NM_147780
ATG4B	2.41E-02	1.23E-03	1.2	**-1.4**	1.2	**1.6**	ENST00000475693	23192	NM_178326
ATG4D	2.66E-02	1.43E-03	-1.0	**1.7**	**2.1**	**1.2**	ENST00000586417	84971	NM_032885
BNIP3L	1.53E-03	1.58E-05	-1.2	-1.2	**-1.9**	**-1.6**	ENST00000620910	665	NM_004331
EVA1A	4.73E-02	3.42E-03	-1.0	**-7.3**	-1.8	**4.1**	ENST00000410113	84141	NM_032181
NSF	9.61E-03	3.02E-04	1.0	**-1.9**	-1.4	**1.4**	ENST00000611398	4905	NM_006178
WIPI2	9.65E-03	3.04E-04	1.2	**-1.2**	**1.4**	**1.6**	ENST00000288828	26100	NM_015610
LAMP1	7.19E-03	1.89E-04	1.0	**-1.7**	**-1.4**	1.2	ENST00000472564	3916	NM_005561
MAP1LC3B	7.25E-03	1.93E-04	-1.2	-1.1	**1.6**	**1.8**	ENST00000556529	81631	NM_022818
SQSTM1	7.84E-03	2.18E-04	1.2	**1.6**	**2.4**	1.5	ENST00000360718	8878	NM_003900
SIRT6	5.17E-03	1.13E-04	1.2	1.1	1.9	1.8	ENST00000600938	51548	NM_016539

Table 2. Changes in fatty acids content, enzyme activity in non-differentiated and differentiated Chub-S7 cells in the presence of saquinavir (SQV 30 μM). The results presented as average (n = 3) concentration in nmol/mg protein of the lipid species and fatty acid detected using mass spectrometry (GS-MS/MS, n = 3) were used for calculation of the product/substrate ratio (enzyme activity) for enzymes associated with fatty acid metabolism.

	ctrl (–)	ctrl (–) + SQV	ctrl (+)	ctrl (+) + SQV
DNL				
18:2/14:0	4.79	6.21	5.43	4.75
SCD1/SCD5				
16:1/16:0	5.06	4.88	4.91	4.59
18:1/18:0	26.91	57.61	30.95	36.68
ELOVL3/ELOVL6				
18:0/16:0	0.99	1.07	0.86	1.20
18:1/16:1	5.80	7.69	3.61	5.45
ELOVL5				
20:3/18:3	5.49	7.35	5.51	5.82
FADS1				
20:4/20:3	1.11	0.89	0.38	0.41
FADS2				
20:3/18:2	3.06	3.50	1.57	1.73
AA/DHA+EPA	1.70	2.21	2.45	2.85
PC/FC	1.29	1.41	1.18	1.49
SFA	2.38	2.30	3.93	3.57
MUFA	8.62	16.06	14.33	19.24
PUFA	12.20	20.14	17.46	26.23

using an assay allowing for the assessment of MDC fluorescence related to the autophagic vacuole formation at the cellular level (*Fig. 4*).

Adding SQV to differentiated Chub-S7 cells significantly increased MDC fluorescence intensity indicating that SQV activated autophagy. It was observed only in differentiated cells, which also confirmed microarray results.

Based on the quantities of incorporated fatty acids the product/substrate ratio of fatty acids (*Table 2*) was used to assess the indirect activity of individual enzymes involved in fatty acids metabolism (27). This activity was correlated with gene expression results derived from analysis of the microarray data (*Table 1*). Differentiation stimulating condition increased the amount of SFA, which is consistent with the observed elevated level of *de novo* lipogenesis - DNL factor (18:2/14:0) and expression of enzymes participating in *de novo* FA synthesis (ACACB, ACAA2, HADHSC, ECHS1, ECHC1, HERC, PERC) (*Table 2*).

Adding SQV to non-differentiated and differentiated Chub-S7 cells resulted in inhibition of *de novo* lipogenesis and increased content of lipid species with MUFA and PUFA. It correlated with calculated enzyme activity of elongases ELOVL3 and ELOVL6 (18:0/16:0, 18:1/16:1), which elongate chains of SFAs and MUFAs with a chain length of 16-22 carbon atoms (*Table 1* and *2*). Despite observed down-regulation of ELOVL5 expression significant increase in PUFA, caused by SQV, was found. This could either be related to the activation of ELOVL5 elongating polyunsaturated fatty acids and FADS2 desaturase responsible for the introduction of an unsaturated bond into the fatty acid molecules during the synthesis of DGLA (dihomo-gamma-linolenic acid) or more probably SQV inhibited PUFA utilization by Chub-S7 cells.

The ratio of 20:4/20:3 for FADS1 indicated that the stimulation of differentiation reduced the amount of arachidonic acid incorporated in lipids, which was described previously (28), while SQV inhibited AA utilization in Chub-S7 cells.

Additionally the influence of SQV on changes in miRNA expression in differentiated Chub-S7 cells was analyzed. The obtained results indicated that among about 700 of analyzed miRNA species only miR-100-3p, miR-222-5p, miR-483-5p were significantly up-regulated.

DISCUSSION

Antiretroviral therapy (ART) is associated with severe symptoms of lipodystrophy, such as peripheral lipoatrophy, central fat accumulation, hyperlipidemia, insulin resistance and hypertension (7, 8). Stopping PIs treatment has not been effective in reducing complications. Body composition involving both abdominal obesity and peripheral lipoatrophy might contribute to the changes in lipids produced by adipose tissue. It has been shown that culture medium of differentiated adipocytes, contained a significant level of methyl palmitate (ADRF) causing aortic vasorelaxation. Decreased ADRF release has been proposed as a factor playing a role in hypertension development (29, 30).

We found that SQV used for anti-HIV therapy inhibited LD formation induced by differentiation conditions, down-regulated expression of genes of PAT proteins adipogenesis markers and enzymes involved in fatty acids metabolism (*Table 1*). This was accompanied by changes in lipid species PI, PEPL, PC and accumulation of MUFA and PUFA (*Table 2*) which suggests autophagy activation. Additionally SQV by increased PC/FC ratio - marker of membrane fluidity (*Table 2*) (31) stimulated production of lipid fractions required for building blocks of membranes needed to form extracellular vesicles (32).

Our results indicated that inhibition of *de novo* lipids production could be associated with activity of ETS1, SREBP, PPARγ and CREB1 transcription factors involved in regulation of expression of fatty acids synthesis and adipogenesis related proteins (*Table1*). It has been described that inhibition of SREBP1 translocation from cytoplasm to nucleus depends on activity of proteases (33). SREBP proteins are produced as membrane-bound precursors located in endoplasmic reticulum. Its translocation to Golgi and following interaction with nuclear lamin A (LMNA) can be blocked by HIV protease inhibitors. Inhibition of LMNA posttranslational modification by zinc metalloprotease ZMPSTE24 affects its interaction with SREBP and then leads to inhibition of adipocyte differentiation (33-35). It was also postulated that SQV related lipodystrophy may be caused by the inhibition of proteins involved in lipid metabolism: CRABP1 and LRP1 that have significant homology to the catalytic site of HIV protease (36), decrease adipocyte CD36 expression and protection apolipoprotein B from degradation by the proteasome (37, 38).

Another suggested reason of PIs side effects such as lipodystrophy includes inhibition of proteasomes activity especially inhibition of the peptidase activity of the 20 S proteasome (39). Accumulation of protein aggregates could stimulate autophagy or apoptosis. Moreover, authors indicated that the protein degradation by proteasome pathway is largely responsible for regulating level of SIRT deacetylases (40). Increased level of SIRTs protein by SQV inhibited proteasome degradation or up-regulated the observed SIRTs gene expression leading to deacetylation of many metabolic enzymes, which were found to be potentially acetylated. Nearly all enzymes involved in glycolysis, gluconeogenesis, the TCA cycle, fatty acid oxidation, the urea cycle, nitrogen metabolism, and glycogen metabolism are acetylated. However deacetylation leads to loss of their activity (41). On the contrary deacetylation of autophagy related proteins stimulates this process (42, 43).

During initiation of autophagy, the formed isolated fragments of membranes recruit lipids from several organelles depending on the cell type and stimulus (44). SQV increased level of PI and PE lipid species participating in autophagosome formation. Formation of isolated membranes from ER depends on PI production and those from mitochondria upon PE (45, 46). SQV related induction of oxidative stress and inhibition of proteasome degradation could activate autophagy by up-regulation of MAP1LC3B gene expression. Moreover, SQV stimulated high level of PUFA, found in our study, could activate autophagy. In contrast, as has been mentioned in other studies, saturated fatty acids such as palmitic acid suppresses autophagy by decreasing membrane fluidity (47-49). The obtained results indicated activation of autophagy by SQV in differentiated Chub-S7 cells through up-regulation of gene expression of proteins participating in different stages of autophagy, which was confirmed by the biological test.

An interrelationship between lipid breakdown and the autophagic pathway was proposed because of observed regulatory and functional similarities between macroautophagy and lipid breakdown or lipolysis (50). Activation of autophagy leads to breakdown of TGs accumulated in LDs (47).

Mitophagy is also induced as an adaptive response, allowing the cell to reduce its mitochondrial mass to limit production of reactive oxygen species in the mitochondria or remove damaged mitochondria (51). Changes in levels of mitochondrial proteins (TOMM20, SLC25A4, HSP60, COX4-IV, electron transport proteins *etc*.) are often used to examine clearance of mitochondria by selective autophagy. The observed decrease of expression of many mitochondrial proteins could indicate that SQV can stimulate two types of autophagy: not only lipophagy (LDs degradation) but also mitophagy (removal of damaged mitochondria).

It has been observed that different ARVs might induce lipid abnormalities, increase insulin resistance and inhibit insulin secretion (52). Our results did not indicate that SQV influences gene expression of proteins participating in insulin receptor pathway in adipocytes. The only significant down-regulation was found for GLUT4 glucose transporter.

Several studies showed SQV related induction of oxidative stress and activation of the expression of pro-inflammatory cytokines by NF-κB (53, 54). Elevated AA/EPA+DHA factor during differentiation with accompanying up-regulation of expression of genes from BCL2 family observed in our study (*Table 1* and *2*) also indicated NF-κB stimulation. SQV enhanced this effect (*Table 1* and *2*). Up-regulation by NF-κB transcription factor BCLN1 expression and disruption of BCLN1/BCL2 complex induced autophagy (55). Activation of NF-κB pathway, ceramide synthesis, increased level of free fatty acids released during lipolysis could induce insulin resistance in adipocytes but also in liver and muscle cells.

A number of strategies for reducing central obesity have been investigated. Changes in diet, exercise, thiazolidinediones, metformin which is presently applied as antidiabetic pharmacotherapy for women with gestational diabetes mellitus, testosterone for men, growth hormone, do not appear to be effective or exert adverse effects (56, 57)

The primary goal of current and future studies is the improved understanding of the mechanisms of and genetic predictions for lipodystrophy so we attempted to look for other targets for therapy. Preliminary analysis of the SQV effect on differentiated CHUB S-7 cells indicated altered miRNA expression - up-regulation of miR-100-3p, miR-222-5p, miR-483-5p. Elevated serum level of miR-483-5p was found in patients with obesity and insulin resistance (58). In β-cells glucose stimulated up-regulation of miR-483-5p increasing insulin secretion. Moreover, miR-483-5p promoted insulin transcription by directly targeting SOCS3 (59). The observed up-regulation of miR-222-5p in adipose tissue leads to activation of lipolysis through inhibition of ETS1, a transcription factor that controls expression of lipid-synthesizing enzymes. As a result, adipocytes release increased amounts of free fatty acids which inhibit insulin signaling in liver and skeletal muscles, inducing peripheral insulin resistance (60). It has been postulated that up-regulation of mir-100-3p inhibits mTOR signaling (61, 62). mTOR is the master regulator that integrates energy status to control growth and metabolism. The down-regulation of mTOR signaling enhances cell viability under ER stress, protects cells against apoptotic death and activates autophagy (63, 64).

Our results indicated that adding SQV to differentiated Chub-S7 cells inhibited expression of genes related to adipocyte differentiation and LD formation. SQV in differentiated Chub-S7 cells by the inhibition of proteasome degradation or excessive ROS generated damaged mitochondria and other cellular components, activating autophagy and removal of lipids deposited in LDs. Additionally SQV in differentiated cells up-regulated micro-RNA, which inhibited adipogenesis, activated autophagy and lipolysis by mTOR inhibition, leading to insulin resistance.

Acknowledgments: Study supported by the grant from The State Committee for Scientific Research no. N N402 421638 and K/ZDS/003774.

Conflict of interests: None declared.

REFERENCES

1. Flexner C. Fat city: understanding HIV lipodystrophy. *Hopkins HIV Rep* 1998; 10: 14-15.
2. Adamson CS, Freed EO. Human immunodeficiency virus type 1 assembly, release, and maturation. In: Advances in

Pharmacology, Vol 55, HIV-1: Molecular Biology and Pathogenesis: Viral Mechanism, Jeang KT (ed). Elsevier Academic Press 2007, pp. 347-387.
3. Ganser-Pornillos BK, Yeager M, Sundquist WI. The structural biology of HIV assembly. *Curr Opin Struct Biol* 2008; 18: 203-217.
4. Olczak A. Metabolic disturbances associated with HAART. *Przegl Epidemiol* 2007; 61: 639-646.
5. Giralt M, Domingo P, Villarroya F. HIV-1 infection and the PPARγ-dependent control of adipose tissue physiology. *PPAR Res* 2009; 2009: 607902. doi: 10.1155/2009/607902.
6. Villarroya F, Domingo P, Giralt M. Drug-induced lipotoxicity: lipodystrophy associated with HIV-1 infection and antiretroviral treatment. *Biochim Biophys Acta* 2010; 1801: 392-399.
7. Haerter G, Manfras BJ, Mueller M, Kern P, Trein A. Regression of lipodystrophy in HIV-infected patients under therapy with the new protease inhibitor atazanavir. *AIDS* 2004; 18: 952-955.
8. Stanley TL, Joy T, Hadigan CM, *et al*. Effects of switching from lopinavir/ritonavir to atazanavir/ritonavir on muscle glucose uptake and visceral fat in HIV-infected patients. *AIDS* 2009; 23: 1349-1357.
9. Caron M, Vigouroux C, Bastard JP, Capeau J. Antiretroviral-related adipocyte dysfunction and lipodystrophy in HIV-infected patients: alteration of the PPARγ-dependent pathways. *PPAR Res* 2009; 2009: 507141. doi:10.1155/2009/507141.
10. Cianflone K, Zakarian R, Stanculescu C, Germinario R. Protease inhibitor effects on triglyceride synthesis and adipokine secretion in human omental and subcutaneous adipose tissue. *Antivir Ther* 2006; 11: 681-691.
11. Flint OP, Noor MA, Hruz PW, *et al*. The role of protease inhibitors in the pathogenesis of HIV-associated lipodystrophy: cellular mechanisms and clinical implications. *Toxicol Pathol* 2009; 37: 65-77.
12. Lagathu C, Kim M, Maachi M *et al*. HIV-antiretroviral treatment alters adipokine expression and insulin sensitivity of adipose tissue in-vitro and in-vivo. *Biochimie* 2005; 87: 65-71.
13. Kim RJ, Wilson CG, Wabitsch M, *et al*. HIV protease inhibitor-specific alterations in human adipocyte differentiation and metabolism. *Obesity* 2006; 14: 994-1002.
14. Garg A, Agarwal AK. Lipodystrophies: disorders of adipose tissue biology. *Biochim Biophys Acta* 2009; 179: 507-513.
15. Tershakovec AM, Frank I, Rader D. HIV-related lipodystrophy and related factors. *Atherosclerosis* 2004; 174: 1-10.
16. Li Vecchi V, Maggi P, Rizzo M, Montalto G. The metabolic syndrome and HIV infection. *Curr Pharm Des* 2014; 20: 4975-5003.
17. Darimont C, Zbinden I, Avanti O, *et al*. Reconstitution of telomerase activity combined with HPV-E7 expression allow human preadipocytes to preserve their differentiation capacity after immortalization. *Cell Death Differ* 2003; 10: 1025-1031.
18. Darimont C, Avanti O, Zbinden I, *et al*. Liver X receptor preferentially activates de novo lipogenesis in human preadipocytes. *Biochimie* 2006; 88: 309-318.
19. Bociaga-Jasik M, Polus A, Goralska J, *et al*. Metabolic effects of the HIV protease inhibitor - saquinavir in differentiating human preadipocytes. *Pharmacol Rep* 2013; 65: 937-950.
20. Ranganathan S, Kern PA. The HIV protease inhibitor saquinavir impairs lipid metabolism and glucose transport in cultured adipocytes. *J Endocrinol* 2002; 172: 155-162.
21. Mauney JR, Volloch V, Kaplan DL. Matrix-mediated retention of adipogenic differentiation potential by human adult bone marrow-derived mesenchymal stem cells during ex vivo expansion. *Biomaterials* 2005; 26: 6167-6175.
22. Leidl K, Liebisch G, Richter D, Schmitz G. Mass spectrometric analysis of lipid species of human circulating blood cells. *Biochim Biophys Acta* 2008; 1781: 655-664.
23. Liebisch G, Lieser B, Rathenberg J, Drobnik W, Schmitz G. High-throughput quantification of phosphatidylcholine and sphingomyelin by electrospray ionization tandem mass spectrometry coupled with isotope correction algorithm. *Biochim Biophys Acta* 2004; 1686: 108-117.
24. Smith PK, Krohn RI, Hermanson GT, *et al*. Measurement of protein using bicinchoninic acid. *Anal Biochem* 1985; 150: 76-85.
25. Kutmon M, van Iersel MP, Bohler A, *et al*. PathVisio 3: an extendable pathway analysis toolbox. *PLoS Comput Biol* 2015; 11: e1004085. doi: 10.1371/journal.pcbi.1004085
26. Barth S, Glick D, Macleod KF. Autophagy: assays and artifacts. *J Pathol* 2010; 221: 117-124.
27. Peter A, Cegan A, Wagner S, *et al*. Hepatic lipid composition and stearoyl-coenzyme A desaturase 1 mRNA expression can be estimated from plasma VLDL fatty acid ratios. *Clin Chem* 2009; 55: 2113-2120.
28. Polus A, Kiec-Wilk B, Czech U, *et al*. Lipid and gene interactions during differentiation of human subcutaneous adipose tissue stromal vascular cells. *J Cell Sci Ther* 2012; 3: 132. doi: 10.4172/2157-7013.1000132
29. Lee YC, Chang HH, Chiang CL, *et al*. Role of perivascular adipose tissue-derived methyl palmitate in vascular tone regulation and pathogenesis of hypertension. *Circulation* 2011; 124: 1160-1171.
30. Deja MA, Malinowski M, Golba KS, Piekarska M, Wos S. Perivascular tissue mediated relaxation - a novel player in human vascular tone regulation. *J Physiol Pharmacol* 2015; 66: 841-846.
31. Owen JS, Bruckdorfer KR, Day RC, McIntyre N. Decreased erythrocyte membrane fluidity and altered lipid composition in human liver disease. *J Lipid Res* 1982; 23: 124-132.
32. van Meer G, Voelker DR, Feigenson GW. Membrane lipids: where they are and how they behave. *Nat Rev Mol Cell Biol* 2008; 9: 112-124.
33. Chang SY, Hudon-Miller SE, Yang SH, *et al*. Inhibitors of protein geranylgeranyltransferase-I lead to prelamin A accumulation in cells by inhibiting ZMPSTE24. *J Lipid Res* 2012; 53: 1176-1182.
34. Lloyd DJ, Trembath RC, Shackleton S. A novel interaction between lamin A and SREBP1: implications for partial lipodystrophy and other laminopathies. *Hum Mol Genet* 2002; 11: 769-777.
35. Coffinier C, Hudon SE, Farber EA, *et al*. HIV protease inhibitors block the zinc metalloproteinase ZMPSTE24 and lead to an accumulation of prelamin A in cells. *Proc Natl Acad Sci USA* 2007; 104: 13432-13437.
36. Carr A. HIV protease inhibitor-related lipodystrophy syndrome. *Clin Infect Dis* 2000; 30: S135-S142.
37. Serghides L, Nathoo S, Walmsley S, Kain KC. CD36 deficiency induced by antiviral therapy. *AIDS* 2002; 16: 353-358.
38. Liang JS, Distler O, Cooper DA, *et al*. HIV protease inhibitors protect apolipiprotein B from degradation by the proteasome: a potential mechanism for protease inhibitor-induced hyperlipidemia. *Nat Med* 2001; 7: 1327-1331.
39. Dong S, Jia C, Zhang S, *et al*. The REGγ proteasome regulates hepatic lipid metabolism through inhibition of autophagy. *Cell Metab* 2013; 18: 380-391.
40. Kanfi Y, Shalman R, Peshti V, *et al*. Regulation of SIRT6 protein levels by nutrient availability. *FEBS Lett* 2008; 582: 543-548.
41. Zhao S, Xu W, Jiang W, *et al*. Regulation of cellular metabolism by protein lysine acetylation. *Science* 2010; 327:1000-1004.

42. Liu J, Wang Y, Li L, *et al*. Site-specific acetylation of the proteasome activator REGγ directs its heptameric structure and functions. *J Biol Chem* 2013; 288: 16567-16578.
43. Shao J, Yang X, Liu T, Zhang T, Xie QR, Xia W. Autophagy induction by SIRT6 is involved in oxidative stress-induced neuronal damage. *Protein Cell* 2016; 7: 2281-90.
44. Benbrook DM, Long A. Integration of autophagy, proteasomal degradation, unfolded protein response and apoptosis. *Exp Oncol* 2012; 34: 286-297.
45. Hailey DW, Rambold AS, Satpute-Krishnan P, *et al*. Mitochondria supply membranes for autophagosome biogenesis during starvation. *Cell* 2010; 141: 656-667.
46. Hayashi-Nishino M, Fujita N, Noda T, Yamaguchi A, Yoshimori T, Yamamoto A. A subdomain of the endoplasmic reticulum forms a cradle for autophagosome formation. *Nat Cell Biol* 2009; 11: 1433-1437.
47. Singh R, Kaushik S, Wang Y, *et al*. Autophagy regulates lipid metabolism. *Nature* 2009; 458: 1131-1135.
48. Koga H, Kaushik S, Cuervo AM. Altered lipid content inhibits autophagic vesicular fusion. *FASEB J* 2008; 24: 3052-3065.
49. Mei S, Ni HM, Manley S, *et al*. Differential roles of unsaturated and saturated fatty acids on autophagy and apoptosis in hepatocytes. *J Pharmacol Exp Ther* 2011; 339: 487-498.
50. Czaja MJ. Autophagy in health and disease. 2. Regulation of lipid metabolism and storage by autophagy: pathophysiological implications. *Am J Physiol Cell Physiol* 2010; 298: C973-C978.
51. Tracy K, Macleod KF. Regulation of mitochondrial integrity, autophagy and cell survival by BNIP3. *Autophagy* 2007; 3: 616-619.
52. van Zoelen MA, Hoepelman AI, de Valk HW. New-onset saquinavir-induced diabetes. *Diabetes Care* 2013; 36: e199. doi: 10.2337/dc13-1645
53. Bubici C, Papa S, Dean K, Franzoso G. Mutual cross-talk between reactive oxygen species and nuclear factor-kappa B: molecular basis and biological significance. *Oncogene* 2006; 25: 731-748.
54. Camandola S, Leonarduzzi G, Musso T, *et al*. Nuclear factor κB is activated by arachidonic acid but not by eicosapentaenoic acid. *Biochem Biophys Res Commun* 1996; 229: 643-647.
55. Grzesiak M, Knapczyk-Stwora K, Slomczynska M. Induction of autophagy in the porcine corpus luteum of pregnancy following anti-androgen treatment. *J Physiol Pharmacol* 2016; 67: 933-942.
56. Sattler FR. Pathogenesis and treatment of lipodystrophy: what clinicians need to know. *Top HIV Med* 2008; 16: 127-133.
57. Zawiejska A, Wender-Ozegowska E, Grewling-Szmit K, Brazert M, Brazert J. Short-term antidiabetic treatment with insulin or metformin has a similar impact on the components of metabolic syndrome in women with gestational diabetes mellitus requiring antidiabetic agents: results of a prospective, randomized study. *J Physiol Pharmacol* 2016; 67: 227-233.
58. Gallo H, Esguerra JS, Eliasson L, Melander O. miR-483-5p associates with obesity and insulin resistance and independently predicts new onset diabetes mellitus and cardiovascular disease. *J Hypertens* 2016; 34: e153.
59. Mohan R, Mao Y, Zhang S, *et al*. Differentially expressed microRNA-483 confers distinct functions in pancreatic beta- and alpha-cells *J Biol Chem* 2015; 290: 19955-19966.
60. Chistiakov DA, Sobenin IA, Orekhov AN, Bobryshev YV. Human miR-221/222 in physiological and atherosclerotic vascular remodeling *BioMed Research International* 2015; 2015: 354517. doi:10.1155/2015/354517
61. Nagaraja AK, Creighton CJ, Yu Z, *et al*. A link between mir-100 and FRAP1/mTOR in clear cell ovarian cancer. *Mol Endocrinol* 2010; 24: 447-463.
62. Pek SL, Sum CF, Lin MX, *et al*. Circulating and visceral adipose miR-100 is down-regulated in patients with obesity and type 2 diabetes. *Mol Cell Endocrinol* 2016; 427: 112-123.
63. Ogata M, Hino S, Saito A, *et al*. Autophagy is activated for cell survival after endoplasmic reticulum stress. *Mol Cell Biol* 2006; 26: 9220-9231.
64. Appenzeller-Herzog C, Hall MN. Bidirectional crosstalk between endoplasmic reticulum stress and mTOR signaling *Trends Cell Biol* 2012; 22: 274-282.

Received: February 8, 2017
Accepted: April 24, 2017

Author's address: Dr. Anna Polus, Department of Clinical Biochemistry, Medical College, Jagiellonian University, 15A Kopernika Street, 31-501 Cracow, Poland.
E-mail: apolus@cm-uj.krakow.pl